Photocatalytic Synthesis of Silver Nanoparticles Stabilized by TiO 2 Nanorods: A Semiconductor/Metal Nanocomposite in Homogeneous Nonpolar Solution

6 AUTHORS, INCLUDING:

Davide Cozzoli
Università del Salento
136 PUBLICATIONS **5,607** CITATIONS

SEE PROFILE

Roberto Comparelli
Italian National Research Council
120 PUBLICATIONS **1,386** CITATIONS

SEE PROFILE

M. L. Curri
Italian National Research Council
245 PUBLICATIONS **3,306** CITATIONS

SEE PROFILE

Angela Agostiano
Università degli Studi di Bari Aldo Moro
357 PUBLICATIONS **4,017** CITATIONS

SEE PROFILE

Photocatalytic Synthesis of Silver Nanoparticles Stabilized by TiO₂ Nanorods: A Semiconductor/Metal Nanocomposite in Homogeneous Nonpolar Solution

P. Davide Cozzoli,[†] Roberto Comparelli,[†] Elisabetta Fanizza,[†] M. Lucia Curri,[‡]
Angela Agostiano,*,[†],[‡] and Danièle Laub[§]

*Contribution from the Dipartimento di Chimica, Università di Bari, Via Orabona 4, 70126 Bari,
Italy, CNR-Istituto per i Processi Chimico Fisici (IPCF), sez. Bari, Via Orabona 4, 70126 Bari,
Italy, and EPFL-CIME-Centre Interdisciplinaire de Microscopie Electronique, Batiment MXC,
1015 Lausanne, Switzerland*

Received November 13, 2003; E-mail: agostiano@area.ba.cnr.it

Abstract: A novel colloidal approach toward semiconductor/metal nanocomposites is presented. Organic-soluble anatase TiO₂ nanorods are used for the first time to stabilize Ag nanoparticles in optically clear nonpolar solutions in the absence of specific ligands for silver. Metallic silver is generated upon UV illumination of deaerated TiO₂ solutions containing AgNO₃. The Ag nanoparticles can be obtained in different size-morphological regimes as a function of the irradiation time, due to light-induced photofragmentation and ripening processes. A mechanism for the colloidal stabilization of the silver nanoparticles is tentatively suggested, which regards the TiO₂ nanorods as inorganic stabilizers, thus acting in the same manner as conventional surfactant molecules. The proposed photocatalytic approach offers a convenient method for producing TiO₂/Ag nanocomposite systems with a certain control over the metal particle size without the use of surfactants and/or additives. Stable colloidal TiO₂-nanorod-stabilized Ag nanoparticles can be potentially available for a number of applications that require "clean" metal surfaces, such as homogeneous organic catalysis, photocatalysis, and sensing devices.

1. Introduction

Nanosized semiconductors and metals[1,2] are extensively studied due to their unusual catalytic and optoelectronic properties, ultimately traceable to the large fraction of atoms residing at the surface compared to the bulk and to confinement of charge carriers inside a small volume of material.

At present, major goals in modern material chemistry are represented by the ability to design, fabricate, and manipulate nanostructured systems to achieve well-tailored chemical–physical characteristics for advanced applications. The wide technological potential offered by low-dimensional inorganic solids is reasonably expected to be even more extended by combining different materials. In particular, metal/semiconductor

oxide composite systems[3–5] are extremely attractive since they represent efficient bifunctional catalysts. In the nanosized regime, specific metal–oxide interactions[3h] can indeed be responsible for the detection of new physical properties or for enhanced catalytic activity, as the oxide can play a precise functional role, thus strongly deviating from its conventional task as a simple support.[3,6,7d] Coupling with noble metals[4,5] has also been demonstrated to increase the photocatalytic and

* Corresponding author.
† Università di Bari.
‡ CNR-IBCF.
§ EPFL-CIME-Centre Interdisciplinaire de Microscopie Electronique.
(1) (a) Wang, Y.; Herron, N. *J. Phys. Chem.* **1991**, *95*, 525. (b) Alivisatos, A. P. *Science* **1996**, *271*, 933. (c) Alivisatos, A. P. *J. Phys. Chem.* **1996**, *100*, 13226. (d) Link, S.; El-Sayed, M. A. *J. Phys. Chem. B* **1999**, *103*, 8410. (e) El-Sayed, M. A. *Acc. Chem. Res.* **2001**, *34*, 257. (f) Kamat, P. V. *J. Phys. Chem. B* **2002**, *106*, 7729.
(2) (a) Schmid, G. *Clusters and Colloids: From Theory to Application.* VCH: Weinheim, Germany, 1994. (b) Kamat, P. V. *Prog. React. Kinet.* **1994**, *19*, 277. (c) Zhang, J. Z. *Acc. Chem. Res.* **1997**, *30*, 423. (d) Kamat, P. V. Composite Semiconductor Nanoclusters. In *Semiconductor Nanoclusters–Physical, Chemical, and Catalytic Aspects*; Kamat, P V., Meisel, D., Eds.; Elsevier Science: Amsterdam, 1997; p 237. (e) Lewis, L. N. *Chem. Rev.* **1993**, *93*, 2693.

(3) (a) Ma, Q.; Klier, K.; Cheng, H.; Mitchell, J. W.; Hayes, K. S. *J. Phys. Chem. B* **2001**, *105*, 9230. (b) Xu, B.-Q.; Wei, J.-M.; Yu, Y.-T.; Li, Y.; Li, J.-L.; Zhu, Q.-M. *J. Phys. Chem. B* **2003**, *107*, 5203. (c) Zhang, F.; Guan, N.; Li, Y.; Zhang, X.; Chen, J.; Zeng, H. *Langmuir* **2003**, *19*, 8230. (d) Dong, W.; Feng, S.; Shi, Z.; Li, L.; Xu, Y. *Chem. Mater.* **2003**, *15*, 1941. (e) Sun, B.; Vorontsov, A. V.; Smirniotis, P. G.; Smirniotis, G. *Langmuir* **2003**, *19*, 3151. (f) Zhang, L.; Yu, C. J.; Yip, H. Y.; Li, Q.; Kwong, K. W.; Xu, A.-W.; Wong, P. K. *Langmuir* **2003**, *19*, 10372. (g) Soejima, T.; Tada, H.; Kawahara, T.; Ito, S. *Langmuir* **2002**, *18*, 4191. (h) Rolison, D. R. *Science* **2003**, *299*, 1698. (i) Bell, A. T. *Science* **2003**, *299*, 1688.
(4) (a) Kamat, P. V.; Flumiani, M.; Dawson, A. *Colloids Surf. A* **2002**, *202*, 269. (b) Dawson, K. A.; Kamat, P. V. *J. Phys. Chem. B* **2000**, 11842. (c) Subramanian, V.; Wolf, E.; Kamat, P. V. *Langmuir* **2003**, *19*, 469. (d) Dawson, A.; Kamat, P. V. *J. Phys. Chem. B* **2001**, *105*, 960. (e) Wood, A.; Giersig, M.; Mulvaney, P. *J. Phys. Chem. B* **2001**, *105*, 8810. (f) Subramanian, V.; Wolf, E. E.; Kamat, P. V. *J. Phys. Chem. B* **2003**, *107*, 7479.
(5) (a) Jakob, M.; Levanon, H.; Kamat, P. V. *Nano Lett.* **2003**, *3*, 353. (b) Chandrasekharan, N.; Kamat, P. V. *J. Phys. Chem. B* **2000**, *104*, 10581. (c) Subramanian, V.; Wolf, E.; Kamat, P. V. *J. Phys. Chem. B* **2001**, *105*, 11439. (d) Stathatos, E.; Lianos, P.; Falaras, P.; Siokou, A. *Langmuir* **2000**, *16*, 2398. (e) Haick, H.; Paz, Y. *J. Phys. Chem. B* **2003**, *107*, 2319. (f) Schmid, G.; West, H.; Mehles, H.; Lehnert, A. *Inorg. Chem.* **1997**, *36*, 891.

photoelectrochemical responses of semiconductor oxides by reducing the fast recombination[8] of the photogenerated charge carriers.

Among the various materials, the well-known TiO_2 and Ag can still offer unexplored opportunities for the realization of novel nanocomposite systems. TiO_2 is the most studied semiconductor[9] for environmental cleanup applications, due to its unique ability in photocatalyzing the degradation of a variety of organic contaminants in wastewater and air and to its chemical inertness and nontoxicity. Silver is an extremely attractive noble metal to be investigated at the nanoscale, due to its remarkable catalytic activity,[6a,7] to its size- and shape-dependent optical properties,[1,10] and to its promising applications in chemical and biological sensing, based on surface-enhanced Raman scattering (SERS),[11] localized surface plasmon resonance (LSPR),[12] and metal-enhanced fluorescence (MEF).[13]

Although several chemical approaches for realizing oxide/metal nanocomposites have been reported, some major limitations emerge, which highlight the urgency of improved preparative routes.

A class of methods comprises the synthesis of oxide-supported metals by reduction of metal precursors inside the voids of porous materials, such as silica, alumina, and zeolites,[6,7d,14] or by dispersion of metal clusters onto oxide powders.[3] Nevertheless, except for a few cases,[3c,d,5d] the use of conventional physical blending or chemical precipitation followed by surface adsorption makes control over the size, morphology, and dispersion of the metal clusters intrinsically difficult.

Another methodology is based on the mixing (either in solution or as deposited films) of preformed metal and oxide nanoparticles.[5] In this regard, colloidal chemistry offers a variety of effective methods for providing metal particles with well-tailored characteristics. Spherical silver nanoparticles have been prepared in solution by either radiolytic,[14e,15a−c] chemical,[10c,11b,15f−l,16] photochemical[10d−g,15d] or photocatalytic reduction[3c,f,g,15n] of silver salts in the presence of a variety of organic stabilizers or inside micelles.[15,17] The preparation of organic-capped Ag particles by electrochemical methods,[18] by laser ablation techniques,[19] and by sonochemical synthesis[20] has also been reported. However, relatively few works have focused on silver sols in nonaqueous media.[15f−i,16b−e] More importantly, while the organic ligands employed in colloidal synthesis are used to affect the solid state and the optical properties of the particles, they can be expected to exhibit susceptibility to chemical oxidation on the surface they protect, especially under photolysis. Another serious limitation is that stabilizers can lead to loss of catalytic activity to a great extent, because they can

(6) (a) Roucoux, A.; Schlz, J.; Patin, H. *Chem. Rev.* **2002**, *102*, 3757. (b) Lewis, L. N. *Chem. Rev.* **1993**, *93*, 2693. (c) Kiwi, J.; Gratzel, M. *J. Am. Chem. Soc.* **1979**, *101*, 7214. (d) Brugger, P. A.; Cuendet, P.; Gratzel, M. *J. Am. Chem. Soc.* **1981**, *103*, 2923. (e) Reets, M, T.; Helbig, W. *J. Am. Chem. Soc.* **1994**, *116*, 7401. (f) Wang, Q.; Liu, H.; Wang, H. *J. Colloid Interface Sci.* **1997**, *190*, 380. (g) Szucs, A.; Berger, F.; Dekany, I. *J. Colloid Interface Sci.* **2000**, *174*, 387.

(7) (a) Jana, N. R.; Sau, T. K.; Pal, T. *J. Phys. Chem. B* **1999**, *103*, 115. (b) Ghosh, S. K.; Kundu, S.; Mandal, M.; Pal, T. *Langmuir* **2002**, *18*, 8756. (c) Pradhan, N.; Pal, A.; Pal, T. *Langmuir* **2001**, *17*, 1800. (d) Claus, P.; Hofmeister, H. *J. Phys. Chem. B* **1999**, *103*, 2766. (e) Sudrik, S. G.; Maddanimath, T.; Chaki, N. K.; Chavan, S. P.; Chavan, S. P.; Sonawane, H. R.; Vijayamohanan, K. *Org. Lett.* **2003**, *5*, 2355. (f) Gang, L.; Anderson, B. G.; Grondelle, J.; van Grondelle, J.; van Santen, R. A. *Appl. Catal. B* **2002**, *40*, 101.

(8) (a) Zhang, Z.; Wang, C. C.; Zakaria, R.; Ying, J. Y. *J. Phys. Chem. B* **1998**, *102*, 10871. (b) Kominami, H.; Muratami, S.; Kato, J.; Kera, Y.; Ohtani, B. *J. Phys. Chem. B* **2002**, *106*, 10501.

(9) (a) *Advanced Catalysis and Nanostructured Materials*; Moser, W. R., Ed.; Academic Press: San Diego, CA, 1990. (b) *Photocatalysis and Environment, Trends and Applications*; Schiavello, M., Ed.; Kluwer: Dordrecht, The Netherlands, 1988. (c) *Photocatalysis. Fundamentals and Applications*; Pelizzetti, E., Serpone, N., Eds.; Wiley: New York, 1989.

(10) (a) Mulvaney, P. *Langmuir* **1996**, *12*, 788. (b) Dickson, R. M.; Lyon, L. A. *J. Phys. Chem. B* **2000**, *104*, 6095. (c) Sun, Y.; Xia, Y. *Science* **2002**, *298*, 2176. (d) Jin, R. C.; Cao, Y. W.; Mirkin, C. A.; Kelly, K. L.; Schatz, G. C.; Zheng, J, G. *Science* **2001**, *294*, 1901. (e) Jin, R.; Cao, Y. C.; Hao, E.; Metraux, G.; Schatz, G. C.; Mirkin, C. A. *Nature* **2003**, *425*, 487. (f) Callegari, A.; Tonti, D.; Chergui, M. *Nano Lett.* **2003**, *3*, 1565. (g) Maillard, M.; Huang, P.; Brus, L. *Nano Lett.* **2003**, *3*, 1611. (h) Zhang, H.; Zelmon, D. E.; Deng, L.; Liu, H.-K.; Teo, B. K. *J. Am. Chem. Soc.* **2001**, *123*, 11300. (i) Wang, W.; Asher, S. A. *J. Am. Chem. Soc.* **2001**, *123*, 12528. (j) Sun, Y.-P.; Riggs, J. E.; Rollins, H. W.; Guduru, R. *J. Phys. Chem. B* **1999**, *103*, 77. (k) Zheng, J.; Dickson, R. M. *J. Am. Chem. Soc.* **2002**, *124*, 13982.

(11) (a) Creighton, J. A.; Blatchford, C. G.; Albrecht, M. G. *J. Chem. Soc., Faraday Trans. 1* **1979**, *75*, 790. (b) Leopold, N.; Lendl, B. *J. Phys. Chem. B* **2003**, *107*, 5723. (c) Liu, Y.; Liu, C.; Zhang, Z.; Wang, C. *Spectrochim. Acta A* **2001**, 35. (d) Franzen, S.; Folmer, J. C. W.; Glomm, W. R.; O'Neal, R. *J. Phys. Chem. A* **2002**, 106, 6533. (e) Kneipp, K.; Kneipp, H.; Itzkan, I.; Dasari, R. R.; Feld, M. S. *Chem. Rev.* **1999**, *99*, 2957. (f) Wenseleers, W.; Stellacci, F.; Meyer-Friedrichsen, T.; Mangel, T.; Bauer, C. A.; Pond, S. J. K.; Marder, S. R.; Perry, J. W. *J. Phys. Chem. B* **2002**, *106*, 6853. (g) Tao, A.; Kim, F.; Hess, C.; Goldberger, J.; He, R.; Sun, Y.; Xia, Y.; Yang, P. *Nano Lett.* **2003**, *3*, 1229.

(12) (a) Malinsky, M. D.; Kelly, K. L.; Schatz, G. C.; Van Duyne, P. *J. Am. Chem. Soc.* **2001**, *123*, 1471. (b) Haes, A. J.; Van Duyne, P. *J. Am. Chem. Soc.* **2002**, *124*, 10596. (c) Hutter, E.; Fendler, J. H.; Roy, D. *J. Phys. Chem. B* **2001**, *105*, 11159.

(13) **(a)** Geddes, C. D.; Cao, H.; Gryczynski, I.; Gryczynski, Z.; Fang, J.; Lakowicz, J. R. *J. Phys. Chem. A* **2003**, *107*, 3443. (b) Nabika, H.; Deki, S. *J. Phys. Chem. B* **2003**, *107*, 9989. (c) Parfenov, I.; Gryczynski, I.; Malicka, J.; Geddes, C. D.; Lakowicz, J. R. *J. Phys. Chem. B* **2003**, *107*, 8829. (d) Selvan, S. T.; Hayakawa, T.; Nogami, M. *J. Phys. Chem. B* **1999**, *103*, 7064.

(14) (a) Shi, H.; Zhang, L.; Cai, W. *Mater. Res. Bull.* **2000**, *35*, 1689. (b) Szucs, A.; Berger, F.; Dekany, I. *Colloids Surf. A* **2000**, *174*, 387. (c) Manninger, I.; Paal, Z.; Tesche, B.; Klngler, U.; Halasz, J., Kiricsi, I. *J. Mol. Catal.* **1991**, 361. (d) Tan, B. J.; Klabunde, K. J.; Sherwood, M. A. *J. Am. Chem. Soc.* **1991**, *113*, 855. (e) Hornebecq, V.; Antonietti, M.; Cardinal, T.; Treguer-Delapierre, M. *Chem. Mater.* **2003**, *15*, 1993.

(15) (a) Gutierrez, M.; Henglein, A. *J. Phys. Chem.* **1993**, *97*, 11368. (b) Henglein, A.; Giersig, M. *J. Phys. Chem. B* **1999**, *103*, 9533. (c) Henglein, A. *Langmuir* **2001**, *17*, 2329. (d) Henglein, A. *Chem. Mater.* **1998**, *10*, 444. (e) Huang, H. H.; Ni, X. P.; Loy, G. L.; Chew, C. H.; Tan K. L.; Loh, F. C.; Deng, J. F.; Xu, G. Q. *Langmuir* **1996**, *12*, 909. (f) Liz-Marzan, L. M.; Tourino, I. L. *Langmuir* **1996**, *12*, 3585. (g) Pastoriza-Santos, I.; Liz-Marzan, L. M. *Langmuir* **1999**, *15*, 948−951. (h) Rodriguez-Gattorno, G.; Diaz, D.; Rendon, L.; Hernandez-Segura, G. O. *J. Phys. Chem. B* **2002**, *106*, 2482. (i) Quaroni, L.; Chumanov, G. *J. Am. Chem. Soc.* **1999**, *121*, 10642. (j) Pal, T.; Sau, T. K.; Jana, N. R. *Langmuir* **1997**, *13*, 1481. (k) Manna, A.; Imae, T.; Aoi, K.; Okada, M.; Yogo, T. *Chem. Mater.* **2001**, *13*, 1674. (l) Zhang, Z.; Patel, R. C.; Kothari, R.; Johnson, C. P.; Friberg, S. E.; Aikens, P. *J. Phys. Chem. B* **2000**, *104*, 1176. (m) Jiang, X.; Xie, Y.; Lu, J.; Zhu, L, He, W.; Qian, Y. *Langmuir* **2001**, *17*, 3795. (n) Hada, H.; Yonezawa, Y.; Yoshida, A.; Kurakate, A. *J. Phys. Chem.* **1976**, *80*, 2728.

(16) (a) Cliffel, D. E.; Zamborini, F. P.; Gross, S. M.; Murray, R. W. *Langmuir* **2000**, *16*, 9699. (b) Wang, W.; Chen, Y.; Efrima, S. *J. Phys. Chem. B* **1999**, *103*, 7238. (c) Wang, W.; Efrima, S.; Regev, O. *Langmuir* **1998**, *14*, 602. (d) Tzahayik, O.; Sawant, P.; Efrima, S.; Kovalev, E.; Klung, J. T. *Langmuir* **2002**, *18*, 3364. (e) Pastoriza-Santos, I.; Liz-Marzan, L. M. *Pure Appl. Chem.* **2000**, *72*, 83. (f) Li, X.; Zhang, J.; Xu, W.; Jia, H.; Wang, X.; Yang, B.; Zhao, B.; Li, B.; Ozaki, Y. *Langmuir* **2003**, *19*, 4285. (g) Burshtain, D.; Zeiri, L.; Efrima, S. *Langmuir* **1999**, *15*, 3050. (h) Mandal, S.; Gole, A.; Lala, N.; Gonnade, R.; Ganvir, V.; Sastry, M. *Langmuir* **2001**, *17*, 6262.

(17) (a) Ohde, H.; Hunt, F.; Wai, C. M. *Chem. Mater.* **2001**, *13*, 4130. (b) McLeod, M. C.; McHenry, R. S.; Beckman, E. J.; Roberts, C. B. *J. Phys. Chem. B* **2003**, *107*, 2693. (c) Bagwe, R. P.; Khilar, K. C. *Langmuir* **2000**, *16*, 905. (d) Taleb, A.; Petit, C.; Pileni, M. P. *Langmuir* **1997**, *9*, 950. (e) Ji, M.; Chen, X.; Wai, C. M.; Fulton, J. *J. Am. Chem. Soc.* **1999**, *121*, 2631.

(18) (a) Rodriguez-Sanchez, L.; Blanco, M. C.; Lopez-Quintela, M. A. *J. Phys. Chem. B* **2000**, *104*, 9683. (b) Yin, B.; Ma, H.; Wang, S.; Chen, S. *J. Phys. Chem. B* **2003**, *107*, 8898. (c) Romanska, D.; Mazur, M. *Langmuir* **2003**, *19,* 4532. (d) Geddes, C. D.; Parfenov, A.; Roll, D.; Fang, J.; Lakowicz, J. R. *Langmuir* **2003**, *19*, 6236.

(19) Mafunè, F.; Kohno, J.; Takeda, Y.; Kondow, T.; Sawabe, H. *J. Phys. Chem. B* **2000**, *104*, 8333.

(20) (a) Pol, V. G.; Srivastava, D. N.; Palchik, O.; Palchik, V.; Slifkin, M. A.; Weiss, A. M.; Gedanken, A. *Langmuir* **2002**, *8,* 3352. (b) Dimitrijevic, N. M.; Bartels, D. M.; Jonah, C. D.; Takahashi, K.; Rajh, T. *J. Phys. Chem. B* **2001**, *105*, 954. (c) Zhu, J.; Liu, S.; Palchik, O.; Koltypin, Y.; Gedanken, A. *Langmuir* **2000**, *16*, 6396.

block a number of active sites,[21] both by strongly interacting with the metal surface and by sterically hindering the access of reactants to the metal surface.

A third approach to nanocomposites involves the creation of core−shell nanostructures either by depositing metal onto colloidal oxide nanoparticles[4] as stabilizers in solution or by growing amorphous oxides (silica or titania) onto properly functionalized metal nanoparticles.[22] Oxide shells have been actually proven to be an efficient means of modulating the optical properties of metal nanoparticles and of providing stability enhancement against light damages. However, although in such nanostructures the metal core is not made catalytically inert by the oxide coating,[22a,b] further confirmations are needed in order to demonstrate their general applicability in catalysis.

In this work, the preparation and the characterization of a novel TiO_2/Ag nanocomposite system are reported. It is shown that organic-soluble anatase TiO_2 nanorods can act as effective stabilizers for segregated Ag nanoparticles in optically clear nonpolar solutions in the absence of specific ligands for silver. Metallic silver is photocatalytically generated upon UV illumination of deaerated TiO_2 solutions containing $AgNO_3$. Alternatively, a two-step approach can be used, in which silver ions are first reduced by sodium borohydride and subsequently irradiated. In both cases, the Ag nanoparticles are obtained in different size-morphological regimes as a function of the illumination time. A mechanism for the colloidal stabilization of the Ag nanoparticles is tentatively proposed, which regards the TiO_2 nanorods as inorganic stabilizers, thus acting in the same manner as conventional surfactant molecules.

The proposed photochemical approach offers a convenient method for producing silver nanoclusters with a certain degree of control over the metal nanoparticle size without employing organic stabilizers and/or additives. A high chemical reactivity characterizes the as-prepared TiO_2-nanorod-stabilized Ag nanoparticles, thus suggesting that they can be potentially used for a number of applications that require "clean" metal surfaces, such as homogeneous catalysis, photocatalysis, and chemical sensing devices.

2. Experimental Section

(2.1) Materials. All chemicals were of the highest purity available and were used as received without further purification. Silver nitrate ($AgNO_3$, 99.998%), sodium borohydride ($NaBH_4$, 98%), titanium tetraisopropoxide ($Ti(OPr^i)_4$ or TTIP, 99.999%), trimethylamino-*N*-oxide dihydrate (($CH_3)_3NO\cdot 2H_2O$ or TMAO, 98%), trimethylamine (($CH_3)_3N$ or TMA, water solution), tetramethylammonium hydroxide (($CH_3)_4NOH$ or TMAH, water solution), tetrabutylammonium hydroxyde (($C_4H_9)_4NOH$ or

TBAH, water solution), anhydrous ethylene glycol ($HO(CH_2)_2$-OH or EG, 99.8%), and oleic acid ($C_{18}H_{33}CO_2H$ or OLEA, 90%) were purchased from Aldrich.

All solvents used were of analytical grade and purchased from Aldrich.

(2.2) Synthesis of TiO_2 Nanocrystals. Organic-capped anatase TiO_2 nanocrystals were synthesized by hydrolysis of TTIP using technical grade OLEA as surfactant at low temperatures (80−100 °C), as reported elsewhere.[23] Briefly, TTIP was hydrolyzed by reacting with an excess of aqueous base solution (H_2O:TTIP molar ratio ranged from 40:1 to 150:1). Various organic bases (TMAO, TMA, TMAH, or TBAH) could be used as catalysts for polycondensation. The morphology of the resulting TiO_2 nanocrystals was modulated by varying the modality of the water supply in the reaction mixture. Rodlike titania nanocrystals were synthesized by direct injection of large aqueous base volumes into OLEA:TTIP mixtures, whereas nearly spherical particles were obtained when water was in situ released from the slow esterification reaction of OLEA and added EG. The TiO_2 nanocrystals were readily precipitated upon addition of an excess of ethanol to the reaction mixture at room temperature. The resulting precipitate was isolated by centrifugation and washed three times with ethanol to remove surfactant residuals. At this stage, the OLEA-coated TiO_2 nanoparticles were easily redispersed in chloroform, without any further growth or irreversible aggregation. A detailed structural and morphological characterization of the as-prepared TiO_2 nanocrystals can be found in ref 23.

In the photocatalytic experiments in this work, freshly capped titania nanocrystals were used. For this purpose, the following procedure was therefore applied. First, the as-prepared OLEA-capped TiO_2 nanocrystals were repeatedly washed until they lost solubility. Then, a volume of 3−4 mL of $CHCl_3$ was added to the precipitate to prepare a turbid suspension. A 0.5 M OLEA solution in $CHCl_3$ was subsequently dropped into the suspension under stirring at room temperature until a clear solution was obtained. The resulting mixture was allowed to stir at room temperature for 90 min, after which ethanol was added to precipitate the nanoparticles again. The TiO_2 nanoparticles were finally washed three times and redissolved in $CHCl_3$ for the photocatalytic experiments.

(2.3) Synthesis of TiO_2/Ag Nanocomposites. (2.3.1) Photocatalytic Synthesis. A quartz cuvette was filled with a solution containing the desired concentration of TiO_2 nanocrystals (expressed with reference to the parent species, TTIP) and $AgNO_3$ in $CHCl_3$:EtOH mixtures (EtOH content was 2−10% (v/v)). $AgNO_3$ concentration ranged between 10^{-6} and 10^{-3} M, while TiO_2 concentration was between 10^{-1} and 10^{-4} M. Both nearly spherical and rodlike TiO_2 nanocrystals were tested as stabilizers for the silver nanoparticles. To obtain a stable nanocomposite (i.e. to prevent the premature precipitation of the silver particles), the TiO_2:$AgNO_3$ molar ratio was kept in the range from 100:1 to 1:1.

The cuvette was sealed by a Teflon-faced rubber cap and subsequently deaerated by gently purging the solution with nitrogen for 30 min. The mixture was UV-irradiated under stirring by using a high-pressure 200 W mercury lamp (λ > 300 nm). The light intensity was adjusted by placing neutral

(21) (a) Kapoor, S. *Langmuir* **1999**, *15*, 4365. (b) Li, Y.; El-Sayed, M. A. *J. Phys. Chem. B* **2001**, *105*, 8938. (c) Narayanan, R.; El-Sayed, M. A. *J. Am. Chem. Soc.* **2003**, *125*, 8340. (d) Jana, N. R.; Wang, Z. L.; Pal, T. *Langmuir* **2000**, *16*, 2457. (e) Schmid, G.; West, H.; Mehles, H.; Lehnert, A. *Inorg. Chem.* **1997**, *36*, 891. (f) Yeung, L. K.; Croooks, R. M. *Nano Lett.* **2001**, *1*, 14.

(22) (a) Ung, T.; Liz-Marzan, L. M.; Mulvaney, P. *Langmuir* **1998**, *14*, 3470. (b) Ung, T.; Liz-Marzan, L. M.; Mulvaney, P. *J. Phys. Chem. B* **1999,** *103*, 6770. (c) Liz-Marzan, L. A.; Mulvaney, P. *J. Phys. Chem. B* **2003**, *107*, 7312. (d) Tom, R. T.; Nair, S.; Singh, N.; Aslam, M.; Nagendra, C. L.; Philip, R.; Vijayamohanan, K.; Pradeep, T. *Langmuir* **2003**, *19*, 3439. (e) Liz-Marzan, L. M.; Giersig, M.; Mulvaney, P. *Langmuir* **1996**, *12*, 4329. (f) Mayya, K. S.; Gittins, D. I.; Caruso, F. *Chem. Mater.* **2001**, *13*, 3833. (g) Guo, Y. G.; Wan, L.-J.; Bai, C. L. *J. Phys. Chem. B* **2003**, *107*, 5441. (h) Li, T.; Moon, J.; Morrone, A. A.; Mecholsky, J. J.; Talham, D.; Adair, J. H. *Langmuir* **1999**, *15*, 4328. (i) Ung, T.; Marzan, L. M.; Mulvaney, P. *J. Phys. Chem. B* **2001**, *105*, 3441.

(23) Cozzoli, P. D.; Kornowski, A.; Weller, H. *J. Am. Chem. Soc.* **2003**, *125*, 14539.

density filters on the light path in order to minimize photooxidation of the TiO$_2$ organic capping, thereby prolonging the temporal stability of the TiO$_2$ colloids under illumination. Aliquots were extracted at scheduled time intervals via a syringe under exclusion of air and properly diluted with deaerated solvent for absorption measurements and for immediate transmission electron microscopy (TEM) investigations. The final color of the solution ranged from pale yellow to dark brown, as the initial AgNO$_3$ content was varied from 10^{-6} to 10^{-3} M, respectively.

(2.3.2) Chemical−Photochemical Two-Step Synthesis. A suspension of NaBH$_4$ in ethanol and a CHCl$_3$ solution of TiO$_2$ nanocrystals containing AgNO$_3$ were prepared in glass vials, then sealed by a Teflon-faced rubber cap, and finally purged with N$_2$ for 30 min. The NaBH$_4$ suspension was added either by drops or in a single portion to the vigorously stirred TiO$_2$/AgNO$_3$ solution via a syringe. The NaBH$_4$:AgNO$_3$ ratio was maintained at near the stoichiometric value. Silver ion reduction was instantaneous, as inferred by the sudden change of the solution from colorless to yellow or dark brown, depending on the total silver concentration. The samples obtained by this procedure could be subsequently transferred to a quartz cuvette and subjected to UV illumination under the same conditions used in the fully photocatalytic method.

(2.4) Characterization of Samples. (2.4.1) UV−Vis Absorption Spectroscopy. UV−vis absorption spectra were recorded with an Ocean Optics UV−vis diode array spectrophotometer equipped with an optical fiber, a deuterium lamp, and a tungsten−halogen lamp.

(2.4.2) Powder X-ray Diffraction. The TiO$_2$ powders for routine X-ray diffraction (XRD) analysis were prepared by precipitating the nanocrystals upon addition of excess ethanol, then by washing the precipitate repeatedly, and finally by evaporating the residual solvent under vacuum at room temperature. XRD patterns were collected with a Philips PW1729 diffractometer in a conventional $\theta-2\theta$ reflection geometry using filtered Cu Kα radiation (λ = 1.540 56 Å). For XRD measurements the nanocrystal powder was placed on an Al sample holder.

(2.4.3) Transmission Electron Microscopy. Transmission electron microscopy images were obtained using a Philips EM 430 microscope (TEM) operating at 300 kV. The samples for the analysis were prepared by dropping dilute solutions of freshly synthesized TiO$_2$/Ag nanocomposite onto 400-mesh carbon-coated copper grids and leaving the solvent to dry. The samples were stable under the electron beam and did not degrade within the typical observation times

3. Results

(3.1) Colloidal Stability of TiO$_2$ Nanocrystals under UV Irradiation. For the photochemical experiments in this work, shape-controlled surfactant-capped anatase TiO$_2$ nanocrystals with high solubility in nonpolar solvents were synthesized by hydrolysis of TTIP in oleic acid.[23] A typical TEM image of the OLEA-capped TiO$_2$ nanorods employed in our photochemical experiments is reported in Figure 1A. The picture shows high-aspect-ratio nanoparticles, having uniform lengths of about 30 nm and diameters of 3−4 nm and appearing well separated on the grid, because of their surface organic coating. The single-

crystal nature of the nanorods and their growth orientation along the *c*-axis direction of the anatase lattice are demonstrated elsewhere.[23]

Preliminary experiments were carried out in order to assess the colloidal photostability of the organic-capped titania nanocrystals in CHCl$_3$ solutions. The formation of suspended floccules was observed after illumination for more than 3−4 h under air atmosphere, depending on the initial titania concentration. A precipitate was ultimately isolated by centrifugation, which could be perfectly redissolved in CHCl$_3$ upon renewed addition of fresh OLEA. Both XRD and TEM analyses confirmed within the experimental error that the collected precipitate was composed of anatase TiO$_2$ nanocrystals whose structural and morphological features were unchanged with respect to those of the un-irradiated material. It was noted that the occurrence of flocculation was delayed to a considerable extent (by 5−6 h) under oxygen-free conditions. Moreover, the addition of small amounts of ethanol (<15% (v/v)) and/or of more OLEA molecules (the OLEA:TiO$_2$ molar ratio was typically varied between 1:1 and 100:1) to the chloroformic titania solution was effective in preserving the photostability of the titania nanoparticles over more than 7−9 h under UV light, depending on the absolute alcohol/OLEA content. In all cases, no noticeable absorption changes were detected during the course of UV irradiation.

(3.2) Synthesis of TiO$_2$/Ag Nanocomposites. In the absence of titania nanoparticles, addition of AgNO$_3$ to CHCl$_3$ gave a turbid suspension, because of the scarce solubility of the silver salt in apolar solvents. In contrast, an optically clear solution was produced upon mixing AgNO$_3$ with TiO$_2$ nanocrystals in chloroform. As a matter of fact, the net amount of AgNO$_3$ that could be dissolved in CHCl$_3$ increased proportionally with the titania concentration. In this respect, rodlike nanoparticles were found extremely effective, as they helped in solubilizing more than 10-fold the AgNO$_3$ amount than spherical particles could do at the same TiO$_2$ concentration. No further organic molecules were intentionally added as complexing agents for Ag$^+$ ions. Accordingly, blank experiments (i.e. without TiO$_2$) showed that even in the presence of deliberately added OLEA molecules (the stabilizer:AgNO$_3$ molar ratio was varied from 1:1 to 10:1), AgNO$_3$ could not be fully solubilized in the apolar medium.

The organic-capped titania nanocrystals were employed to provide UV-photogenerated electrons for Ag$^+$ reduction as well as to act as support for Ag deposition in the absence of specific organic capping agents for metal silver. The photoreduction experiments were performed at room temperature in deaerated CHCl$_3$, while a fixed ethanol content (10% (v/v)) was ensured in the solution in order to prevent precipitation of the titania nanocrystals. Due to the excellent colloidal stability of the nanocomposites based on TiO$_2$ nanorods, unless otherwise stated, we will refer to preparations carried out with rodlike titania nanocrystals.

Prolonged (>4 h) UV irradiation of AgNO$_3$ suspensions in the absence of titania exclusively led to scarce pale-yellow deposits sticking onto the inner walls of the cuvette. By comparison, upon illumination of TiO$_2$/AgNO$_3$ solutions, stable colloidal solutions were readily obtained which exhibited the progressive evolution of the characteristic silver surface plasmon (SP) band in the 350−500 nm spectral region, being indicative of the formation of nanometer-sized metal clusters.[1,10] Because
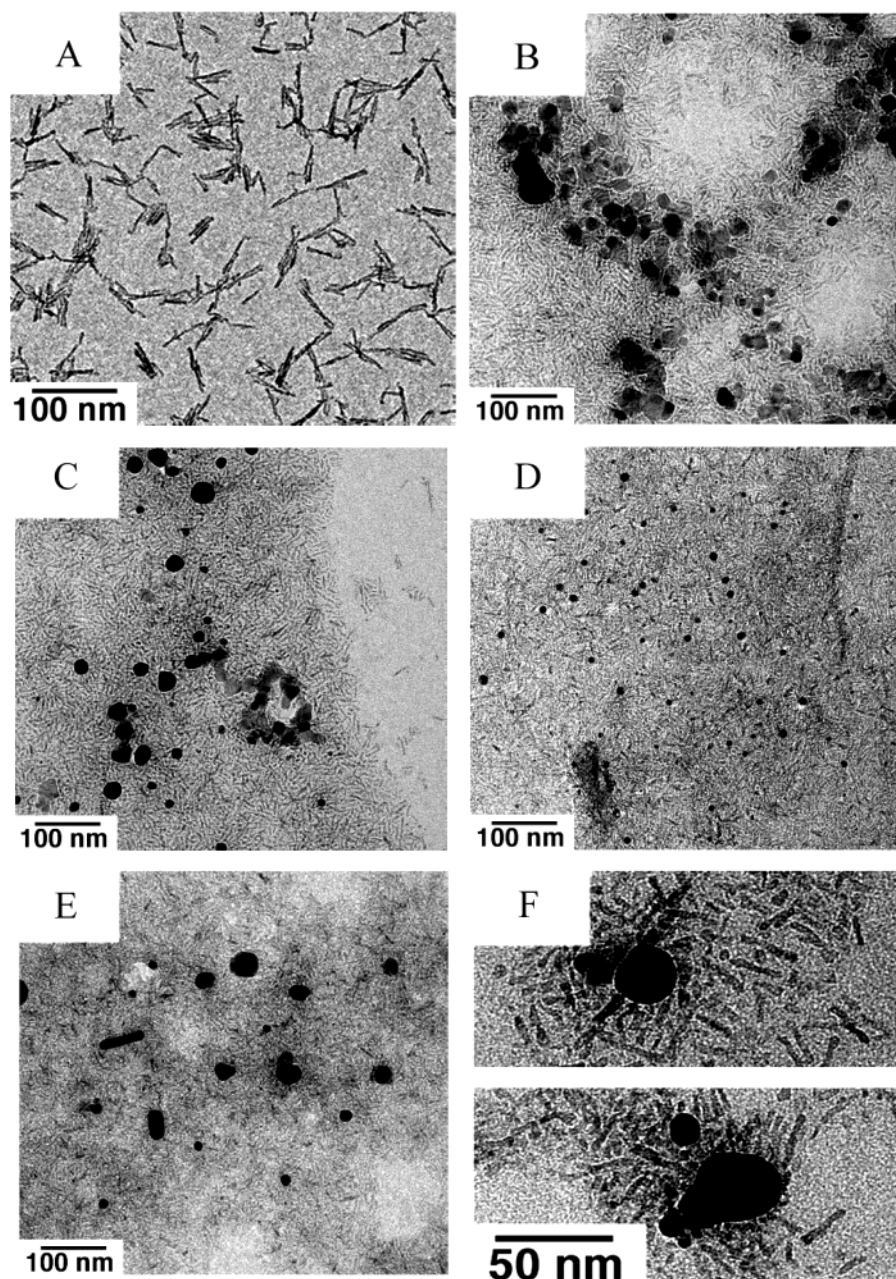
Figure 1. TEM overview of (A) OLEA-capped TiO$_2$ nanorods; (B−E) photocatalytically prepared TiO$_2$ nanorod/Ag nanocomposites extracted from the same reaction batch at different irradiation times. The corresponding absorption spectra are shown in Figure 2a,b,d,f,g, respectively. (F) Characteristic assemblies of individual Ag nanoparticles and TiO$_2$ nanorods.

of the intense absorption of silver sols at concentrations higher than 10^{-4} M, the evolution of the silver SP band was followed by measuring the absorption spectrum of aliquots extracted from the mother solution at different illumination stages and subsequently diluted by the same factor with deaerated CHCl$_3$:EtOH.

In Figure 2 the typical temporal evolution of the absorption spectrum of a N$_2$-saturated TiO$_2$ nanorods/AgNO$_3$ solution is reported as a function of the UV-illumination time. Before irradiation, the typical steep and unstructured absorption of titania nanoparticles was seen below 350 nm, with a negligible tail in the visible region (curve a). Such optical features remained unchanged in the dark. At the early stages of the photoreaction, a featureless absorption grew up, which extended up to 700 nm (curves b,c). Subsequently, an asymmetric but well-defined broad SP plasmon band developed with an absorption maximum λ_{max} at 450 nm (curve d). In the successive stages of the

photoreaction, a more symmetric SP band was detected, which simultaneously exhibited a remarkable jump in magnitude, a narrowing of the bandwidth, and a pronounced blue-shift of λ_{max} to around 400 nm (curves e,f). Finally, further illumination red-shifted the SP λ_{max} to around 430 nm (curve g) with a concomitant band broadening and intensity decrease.

Notably, in aerated titania solutions (data not shown), the evolution of the silver plasmon band was characterized by a transient growth over a total time period that varied from 8 to 10 min to about 1 h, depending on the initial AgNO$_3$ concentration. In this case, a broad SP band centered around 450 nm was seen at the very beginning of irradiation. A progressive blue shift of the absorbance maximum with a simultaneous decrease of the SP band intensity followed, ultimately evolving toward the complete SP bleaching, while the solution remained optically transparent.
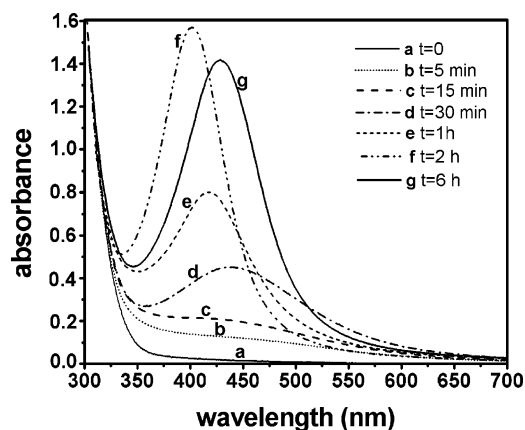
Figure 2. Time-dependent evolution of the absorption spectrum of a TiO₂ nanorods/AgNO₃ solution ([AgNO₃] = 10^{-3} M, [TiO₂] = 5×10^{-2} M) in N₂-saturated CHCl₃:EtOH (90:10 (v/v)) upon UV irradiation. The absorption spectra were recorded on 1:20 diluted aliquots immediately after their withdrawal.

The morphological transformation of the deposited silver clusters in the photosynthesized nanocomposites was investigated by extracting aliquots from the same TiO₂ nanorod/Ag solution at different illumination times and imaging them by TEM. Pats B−E of Figure 1 are representative TEM images of the TiO₂ nanorods/Ag nanocomposite whose absorption spectra correspond to Figure 2b,d,f,g, respectively. The silver clusters were generally found to be associated with areas of the TEM grid that were overcrowded with titania nanocrystals. Because of the significantly lower image contrast characterizing TiO₂ when compared to Ag, the silver nanoparticles could be easily identified as dark spots superimposed on an underlying titania background, as confirmed by energy dispersive analysis of X-rays (EDAX). Electron diffraction pattern analysis also revealed that the samples contained metallic silver and anatase titania. As a general feature, the samples consisted of a mixture of TiO₂ nanorods and segregated silver particles. As opposed to the titania nanoparticles, the Ag particles appeared in different dimensional and/or morphological regimes during the course of illumination. At the early stages of AgNO₃ photoreduction (Figure 1B), relatively large and highly agglomerated Ag clusters were detected, comprising irregularly faceted particles whose sizes ranged from about 60 to 15 nm. Upon continuing UV irradiation (Figure 1C), well-separated but widely polydispersed Ag particles could be observed. At this point, the largest particles had a reduced mean size (up to 35 nm) with respect to the previous stage, while the fraction of smaller clusters (15−20 nm) had slightly increased. Subsequently (Figure 1D), relatively uniform silver particles with a much smaller mean size (8−12 nm) were observed. At the late stages of photolysis (Figure 1E), an increase in the silver mean particle size was apparent (20−50 nm), while a minor fraction of rodlike Ag particles was also observed.

In Figure 1F two representative TEM images are reported showing individual Ag particles in the presence of approximately a monolayer of TiO₂ nanorods on the TEM grid. The titania particles appear to be interacting quite effectively with the silver nanoparticles. Interestingly, many nanorods can be found while orienting their shorter side toward the surface of the silver clusters. Such kinds of assemblies were commonly observed during TEM investigation at all stages of photolysis, whereas TiO₂-unsupported Ag particles (i.e. noninteracting with nano-

rods) were very rarely found even in samples deposited from extremely diluted TiO₂/Ag solutions at relatively low TiO₂:Ag molar ratio.

It deserves to be mentioned that, although the overall optical−morphological evolution proceeded over progressively longer irradiation times with increases in the starting AgNO₃ concentration, the observed variations generally resembled the representative behavior reported in Figures 1 and 2.

Stable TiO₂/Ag nanocomposites were successfully prepared also by applying a mixed chemical−photochemical approach. To make the results comparable with those of the previous method, the concentrations of TiO₂, AgNO₃, and ethanol were kept the same as those used for the fully photoreductive experiments. In the first step, the silver ions were reduced by NaBH₄. After injection of the reductant, the resulting clear solution exhibited a rather broad silver plasmon band, centered at 430−440 nm. TEM analysis revealed that the freshly prepared Ag particles, although less aggregated, were relatively large and polydispersed, as in Figure 1B. In the second step, the freshly prepared sample was subjected to UV irradiation under N₂. Spectral changes occurred which were qualitatively very similar to those reported in Figure 2. Accordingly, TEM showed that the NaBH₄-derived Ag nanoparticles underwent a progressive size−shape transformation closely resembling that reported in Figure 1B−E.

The as-obtained TiO₂/Ag nanocomposite solutions, regardless of the reduction method used, were always optically transparent and exhibited colloidal stability for several weeks under inert atmosphere at room temperature, provided that the TiO₂ nanorod:Ag molar ratio (referred to the parent species, TTIP and AgNO₃, respectively) was kept higher than 1. Below this limiting value, partial precipitation of the sole silver particles was, in fact, slowly occurred after 1−2 days of storage. The same drawback generally was detected when spherical TiO₂ nanocrystals were used as stabilizers. In both cases, the precipitated Ag fraction could not be redispersed again in CHCl₃ after isolation from the solution, unless renewed addition of TiO₂ nanocrystals was carried out.

To investigate the role of the organic-capped titania nanorods as stabilizers for the silver particles, the following experiments were carried out.

Selective precipitation of the silver particles from stable nanocomposites was attempted by dropwise addition of a polar solvent (methanol or ethanol), according to conventional nonsolvent-based procedures to induce the precipitation of colloidal nanocrystals from nonpolar solutions. However, when the limit for the precipitation of the nanocomposite was reached (>50% (v/v) EtOH or MeOH excess), a precipitate was collected by centrifugation which contained both silver and titania nanoparticles and that could be redispersed again in CHCl₃.

To exclude that the organic ligands desorbing from the surface of the titania nanorods (i.e. OLEA) participated in the colloidal stabilization of Ag clusters, AgNO₃ photoreduction was carried out in the presence of OLEA as exclusive stabilizer at a ligand: AgNO₃ molar ratio in the range of 1:1−20:1. Sodium borohydride, UV-photogenerated ketyl radicals in the presence of 2-propanol and acetone,[15d] or UV-photogenerated electrons from an illuminated TiO₂ nanorod thin film deposited onto a quartz substrate were alternatively employed as reductants to produce silver metal particles. As a matter of fact, Ag⁺ reduction in the
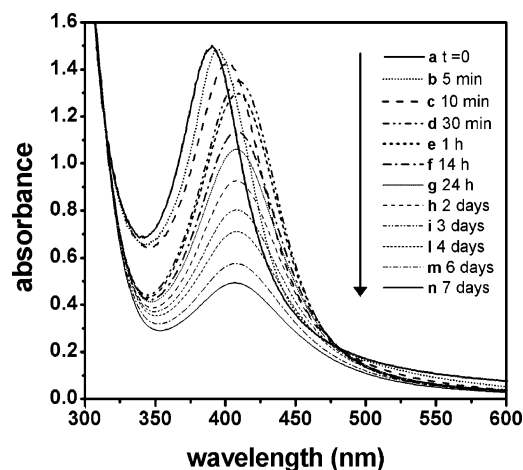
Figure 3. Representative time-dependent evolution of the absorption spectrum of a preformed TiO$_2$ nanorods/Ag solution upon air storage in the dark. The spectra were recorded on 1:20 diluted aliquots extracted from the mother batch ([Ag] $=10^{-3}$ M; [TiO$_2$] $= 5 \times 10^{-2}$ M; CHCl$_3$:EtOH, 90:10 (v/v); 2 h preillumination time).

Figure 4. Effect of excess NaBH$_4$ addition under N$_2$ on the absorption spectrum (curve a) of a photocatalytically prepared TiO$_2$ nanorods/Ag nanocomposite. The spectra were recorded on 1:20 diluted aliquots extracted from the mother batch ([AgNO$_3$] $= 10^{-3}$ M; [TiO$_2$] $= 5 \times 10^{-2}$ M; 25 min irradiation time under N$_2$) at [NaBH$_4$] $= 5 \times 10^{-2}$ M.

presence of the surfactant molecules yielded unstable colloidal metal particles that precipitated within a few hours or remained stuck onto the quartz cuvette walls.

We emphasize that the amount of the employed surfactants for the above-mentioned experiments was actually far exceeding the total ligand content that could be found in the experiments carried out in the presence of TiO$_2$ nanorods. In the TiO$_2$-stabilized Ag colloids, the total organic stabilizer concentration was approximately dictated by the overall amount of organic ligands bound to the titania surface, as the TiO$_2$ nanocrystals were thoroughly washed after surface processing prior to their employment in the photoreduction experiments. It could be also assumed that the establishment of a reversible adsorption–desorption equilibrium of the ligands at the titania surface supplied only a negligible concentration of surfactant molecules in the bulk solution.

(3.3) Chemical Reactivity of the Nanocomposites. (3.3.1) Effect of Oxygen. The temporal stability of the photocatalytically prepared nanocomposites was examined by monitoring the optical changes taking place upon exposing the colloidal solution to air in the dark. In Figure 3, as an example, the temporal evolution of the silver plasmon band of a preformed TiO$_2$/Ag nanocomposite solution is reported as a function of the exposure time to air. In the earliest minutes, the Ag plasmon band was seen to red-shift and to decrease in intensity, after which a continuous band dampening occurred more slowly with a simultaneous and progressive blue-shift of λ_{max}. When the solution was deaerated again by purging with N$_2$, the spectrum did not recover the starting features, thus demonstrating that effects caused by oxygen were not reversible. This behavior was generally observed regardless of the initial silver particle size in the prepared nanocomposite.

(3.3.2) Excess NaBH$_4$ Addition. In Figure 4 the effect of the addition of excess borohydride (10-fold excess with respect to the starting AgNO$_3$ concentration) to a preformed TiO$_2$/AgNO$_3$ solution ([AgNO$_3$] $= 10^{-3}$ M; [TiO$_2$] $= 5 \times 10^{-2}$ M; UV-irradiation time, 25 min) is shown. The manipulations were carried out under N$_2$. The initial TiO$_2$/Ag nanocomposite exhibited spectrum a. Upon NaBH$_4$ powder addition under vigorous stirring, the colloidal nanocomposite turned clear in a
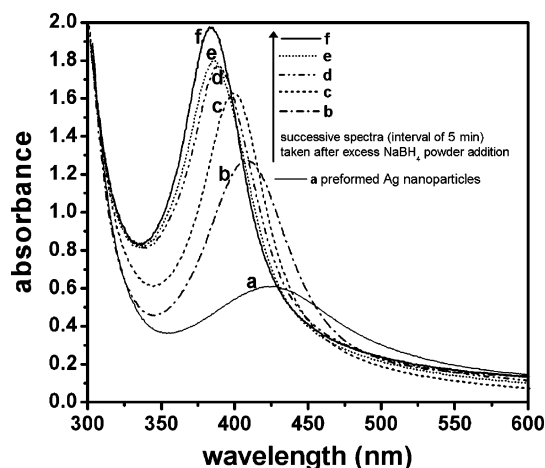
few seconds, while a blue shift, band sharpening, and an increase in the band intensity took place simultaneously (curves b–f). The final λ_{max} value for the plasmon band (curve f) was found at wavelengths below 400 nm. Upon admission of air, the SP band evolved as in Figure 3, however at a significantly slower rate.

(3.3.3) Effect of Ag$^+$ Ion Addition. Upon addition of a relatively high AgNO$_3$ concentration to preformed TiO$_2$/Ag colloids, an initial red shift and a decrease in intensity were initially observed, after which the SP band remain unaltered for a long time.

(3.3.4) Effect of UV Light under Air. The fast (in a few tens of minutes) decrease of the silver SP band was obtained upon UV illumination of preformed TiO$_2$/Ag nanocomposite under air atmosphere, ultimately leading to the complete SP bleaching.

Notably, all the above-mentioned optical changes occurred while the solution remained optically transparent.

4. Discussion

(4.1) TiO$_2$ Photoreactions in Organic Media. Most aspects of the photocatalytic reactions involving titania particulate have been extensively studied in aqueous media.[9,24–26] Photoexcitation of TiO$_2$ generates strongly oxidative ($E^0 = +2.7$ V vs NHE at pH 7) valence band (VB) holes (h$_{VB}^+$) and moderately
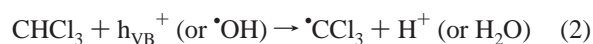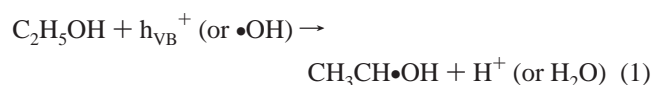
(24) (a) Choi, W.; Hoffmann, M. R. *Environ. Sci. Technol.* **1997**, *31*, 89. (b) Kormann, C.; Bahnemann, D. W.; Hoffmann, M. R. *Environ. Sci. Technol.* **1991**, *25*, 494. (c) Choi, W.; Hoffmann, M. R. *J. Phys. Chem.* **1996**, *100*, 12161 (d) Stark, J.; Rabani, J. *J. Phys. Chem B* **1999**, *103*, 8524. (e) Mills, A.; Le Hunte, S. *J. Photochem. Photobiol. A* **1997**, *108*, 1. (f) Hoffman, M. R.; Martin, S. T.; Choi, W.; Bahnemann, D. F. *Chem. Rev.* **1995**, *95*, 69.

(25) (a) Colon, G.; Hidalgo, M. C.; Navio, J. A. *Langmuir* **2001**, *17*, 7174. (b) Colon, G.; Hidalgo, M. C.; Navio, J. A. *J. Photochem. Photobiol.* **2001**, *138*, 79. (c) Sato, S.; Ueda, K.; Kawasaki, Y.; Nakamura, R. *J. Phys. Chem. B* **2002**, *106*, 9054. (d) Tada, H.; Teranishi, K.; Ito, S. *Langmuir* **1999**, *15*, 7084. (e) Choi, W.; Hoffmann, M. R. *Environ. Sci. Technol.* **1995**, *29*, 1646. (f) The potential is calculated from the polarographic half-wave potential, $E_{1/2} = -0.94$ V vs NHE for the half-reaction of CH$_3$CHO + e$^-$ + H$^+$ → CH$_3$CH·OH and $E^0 = +0.19$ V for the half-reaction of CH$_3$CHO + 2e$^-$ + 2H$^+$ → C$_2$H$_5$OH. See also ref 25e.

(26) (a) Lowekamp, J. B.; Rohrer, G. S.; Morris Hotsenpiller, P. A.; Bolt, J. D.; Farneth, W. E. *J. Phys. Chem. B* **1998**, *102*, 7323. (b) Morris Hotsenpiller, P. A.; Bolt, J. D.; Farneth, W. E.; Lowekamp, J. B.; Rohrer, G. S. *J. Phys. Chem. B* **1998**, *102*, 3216. (c) Farneth, W. E.; McLean, R. S.; Bolt, J. D.; Dokou, E.; Barteau, M. A. *Langmuir* **1999**, *15*, 8569. (d) Wilson, J. N.; Idriss, H. *J. Am. Chem. Soc.* **2002**, *124*, 11284.

reductive ($E^0 = -0.5$ V vs NHE at pH 7) conduction band (CB) electrons (e_{CB}^-) that, in turn, originate highly reactive hydroxyl radicals ($^{\bullet}$OH) and secondary oxidants ($HO_2^{\bullet}$, H_2O_2) in the presence of dissolved oxygen (O_2). Reactions with substrates are dominated by these species, although direct oxidation and reduction by trapped VB holes[24a,25c,d] and by CB electrons,[3c,e,4c,5d,25a,26] respectively, have also been reported.

The present photocatalytic synthesis of Ag nanoparticles was carried out under deaerated conditions in the presence of surfactant-capped TiO_2 nanocrystals in apolar media. In the following qualitative discussion, we approximate[27] the standard redox potential E^0 for some half-reactions to the corresponding half-wave potential value $E_{1/2}$ present in the literature data, as it has been often practiced by other authors.[15d,25e,f,28a,b] We also assume that the literature redox potential scale, measured for aqueous media, is valid for our system.

In deaerated organic solutions, the involved photochemistry can be expected to involve peculiar characteristics with respect to that in aqueous media. First, $^{\bullet}$OH hydroxyl radicals can be supplied only by oxidation of H_2O traces in the solvents, of surface titanol groups, or of TiO_2 surface-adsorbed H_2O, resulting from the hydrolytic synthesis of titania. All these $^{\bullet}$OH sources can therefore be assumed to be scarce. Second, the formation of $HO_2^{\bullet}$ and H_2O_2 can be largely suppressed because of oxygen-free conditions. Finally, the photogenerated holes are expected to react with the organic solvents:

$$C_2H_5OH + h_{VB}^+ \text{ (or } {\bullet}OH) \rightarrow$$
$$CH_3CH{\bullet}OH + H^+ \text{ (or } H_2O) \quad (1)$$

$$CHCl_3 + h_{VB}^+ \text{ (or } {}^{\bullet}OH) \rightarrow {}^{\bullet}CCl_3 + H^+ \text{ (or } H_2O) \quad (2)$$

Especially alcohols[28a,b] with α-hydrogens are known to easily form α-hydroxyalkyl radicals (eq 1) upon α-H atom abstraction. As the half-wave potential, $E^0_{1/2}$, for the couple $CH_3CH^{\bullet}OH/C_2H_5OH$ is $+1.13$ V vs NHE,[25f] there indeed exists a large driving force for hole transfer to ethanol. Moreover, the $CH_3CH^{\bullet}OH$ radicals can further inject electrons into the TiO_2 conduction band or reduce other species, as $E^0_{1/2}$ for the $CH_3CHO/CH_3CH^{\bullet}OH$ couple is -0.94 V (vs NHE).[25e]

In summary, reductive reactions can be strongly enhanced in deaerated $CHCl_3$/EtOH mixtures when compared to aqueous media, because of the efficient hole scavenging by the solvent and the action of reducing radicals in addition to that of e_{CB}^- which escape recombination.

The preliminary photoirradiation experiments on the sole TiO_2 nanocrystals proved that the titania nanoparticle solubility was affected by UV irradiation. However, the precipitated nanoparticles could be redispersed upon fresh addition of OLEA, thus demonstrating that no irreversible aggregation had occurred during their precipitation. Since the titania nanoparticles did not undergo any light-induced structural modifications, the loss of solubility can be accounted for by UV-induced degradation of the organic capping at their surface. Carboxylic acids[25,28b] are actually known to be photooxidized over TiO_2, as in some cases such molecules have been even employed as sacrificial electron

donors to enhance photoreductive reactions.[25d,e] The more facile photodegradation of the capping ligands under ambient atmosphere clearly indicates that electron scavenging by oxygen enhances the oxidation probability of the surface ligands, possibly due to an increase in the hole lifetime and/or to the additional oxidative contribution by $HO_2^{\bullet}$ and H_2O_2.

In mixed $CHCl_3$:EtOH solutions (at EtOH concentration that was, however, far below the limit for inducing oxide precipitation[23] by nonsolvent destabilization), the surfactant-capped titania nanoparticles retained their colloidal stability for a much longer time, due to the slower degradation of the surface coating. In this regard, the significantly high EtOH to surface-ligand molar ratio can be invoked as being responsible for an efficient hole scavenging by the alcohol molecules, thereby retarding the oxidation of the organic stabilizers. Accordingly, the same beneficial effect was obtained upon addition of an excess of OLEA molecules, which apparently ensured a reservoir of capping ligands in the reaction environment, thus compensating for the progressive photooxidative loss of surfactant on the TiO_2 surface.

It deserves to be emphasized that, in view of a general application of organic-soluble titania/metal nanocomposite in steady-state photocatalysis, their colloidal stability is desirable to be preserved as long as possible in order both to sustain prolonged UV irradiation and/or to allow for catalyst recycling. In this respect, the potential for surface-ligand exchange offered in the reversible coordination of OLEA on the TiO_2 nanocrystal surface[23] could stimulate a different engineering of the TiO_2 nanocrystal external coating in two possible directions. One possibility might be the use of other surface ligands which would be more resistant to photocatalytic oxidation. Alternatively, the choice of ligands with suitable functionalities providing titania solubility in polar solvents would allow one to perform photocatalytic experiments directly in ethanol, thus guaranteeing an efficient hole scavenging by the alcohol molecules.

(4.2) Photocatalytic Synthesis and Mechanism for Colloidal Stabilization of Ag Nanoparticles. All the above observations suggested that the organic-capped TiO_2 nanocrystals in deaerated $CHCl_3$/EtOH mixtures could be suitable candidates to act both as a source of reducing species for Ag^+ ions and as a metal support. Upon UV-light irradiation, the deposition of metal silver occurred, as revealed by TEM (Figure 1B–E) and by absorption spectrophotometry (Figure 2). Although metal silver could be photochemically produced to a small extent with no TiO_2 in the presence of alcohols,[15n] the photocatalytic nature of the reduction process involving the UV-excited TiO_2 nanoparticles was apparent from the experimental observations. An inert atmosphere was a stringent requirement to facilitate Ag^+ reduction by the formed reducing species, according to

$$Ag^+ + e_{CB}^- \rightarrow Ag^0 \quad (3a)$$

$$Ag^+ + CH_3CH{\bullet}OH \rightarrow Ag^0 + CH_3CHO + H^+ \quad (3b)$$
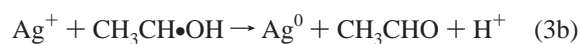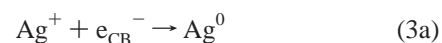
Despite e_{CB}^- consumption during $CHCl_3$ reductive degradation,[24] silver ion reduction ($E^0_{Ag+/Ag} = +0.799$ V) readily proceeded because it is thermodynamically allowed. However, the contribution of reaction 3b to the overall reduction should be much lower than that of reaction 3a, as the deposition rate

(27) Kolthoff, I. M.; Lingane, J. L. *Polarography*; Wiley: New York, 1952.
(28) (a) Kamat, P. V.; Bedja, I.; Hotchandani, S. *J. Phys. Chem.* **1994**, *98*, 9137. (b) Vinodgopal, K.; Bedja, I.; Hotchandani, S.; Kamat, P. V. *Langmuir* **1994**, *10*, 1767. (c) Safrany, A.; Gao, R.; Rabani, J. *J. Phys. Chem. B* **2000**, *104*, 5848.

was almost unchanged in the absence of ethanol. The transfer of photogenerated electrons to surface-bound Ag^+ initiates a process of alternating electron transfer and ion adsorption, which can allow the growth of Ag particles with high quantum yield.[29]

The transient formation of metal silver was detected during irradiation of aerated $TiO_2/AgNO_3$ solution. Furthermore, when preformed TiO_2/Ag nanocomposites were UV-illuminated under air, the silver SP disappeared progressively. These facts demonstrate that, although hole scavenging by ethanol is beneficial toward reactions 3a and 3b, Ag dissolution (eq 4) progressively becomes the dominant process in the presence of oxygen:

$$Ag^0 + h_{VB}^+ \rightarrow Ag^+ \qquad (4)$$
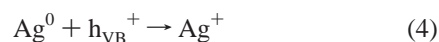
The efficient e_{CB}^- scavenging by dissolved oxygen can, in fact, result both in a decreased number of e_{CB}^- for Ag^+ photoreduction and in a higher availability of h_{VB}^+.

The results of our experiments indicate that TiO_2 nanocrystals with a rodlike morphology are extremely effective in stabilizing silver particles in an apolar media in the absence of either specific ligands for silver or bifunctional cross-linkers[30][30] that keep the oxide and the metal particles in close proximity. In earlier preparations of metal-capped oxide colloids,[4c−f] oxide nanoparticles were employed which carried a surface charge of opposite sign with respect to that of the metal ion precursor, thus favoring its adsorption on the particles. Similarly, the surface of the TiO_2 nanoparticles used in this work may likely be characterized by a significant density of deprotonated titanol groups, as hydrolysis of TTIP was catalyzed by water-soluble organic bases.[23] Accordingly, the upper limit for solubility was, indeed, proportional to the titania concentration in $CHCl_3$, but it was not affected by the presence of surfactants. All of this experimental evidence undoubtedly indicates that electrostatic interactions between Ag^+ ions and the TiO_2 surface are mainly responsible for uniformly solubilizing $AgNO_3$ in nonpolar solutions.

On the other hand, OLEA molecules desorbing from the TiO_2 nanoparticles surface cannot be regarded as the actual stabilizers for the resulting Ag nanoparticles, because these surfactants have been demonstrated to be ineffective in providing stable silver colloids even at high surfactant:Ag molar ratio. Without TiO_2, electrostatic repulsion between homologous surface charges and/ or weak ligand, adsorption cannot prevail over the tendency of metal particles to agglomerate. On the other hand, although long-chain unsaturated carboxylates have been successfully employed to cap silver nanoparticles in aqueous media and to facilitate their transfer into organic solvents,[16b,e] their protonated counterparts can be, in fact, unlikely to serve in the same manner. These observations undoubtedly point to the peculiar involvement of the titania nanocrystals in the stabilization process of the silver nanoparticles.

As a general feature, irrespectively of the used reduction method (either chemical or photocatalytic), our synthetic procedure always yielded a mixture of TiO_2 nanocrystals and segregated silver nanoparticles (Figure 1B−E). This result

represents a remarkable difference when compared to earlier preparations of metals supported by colloidal TiO_2[4b−d] or ZnO[4e,f] nanoparticles. In those cases, the metal ion reduction, in fact, resulted in the deposition of small metallic islands on the oxide surface or in a discontinuous metal shell covering the oxide core. As similar [oxide]:[metal salt] ratios (based on molecular concentrations) were employed in our preparations, metal-covered oxide nanostructures were expected to be found as well, especially at very high concentration of oxide supporting particles, as a result of the decreased Ag nucleation probability in the bulk solution. Such a metal coverage should form even more feasibly by the photoreductive approach, in which direct e_{CB}^- uptake by $AgNO_3$ is likely to take place at the TiO_2 surface. However, since TiO_2 nanocrystals with an extensive metal coverage were never detected, it is believed that an important role in affecting the morphology of metal deposits is indirectly played by the organic layer on the titania nanoparticles. Surfactants adsorbed onto the TiO_2 surface can strongly limit the number of available sites for Ag to nucleate. The metal nuclei could be eventually prevented from further growing as extended islands in the proximity of the oxide surface, because of the sterical hindrance posed by the titania surface ligands. On the other hand, if a uniform thick metal coverage grew onto the titania nanorods, the resulting core−shell nanoparticles should precipitate, their colloidal stability being, in fact, exclusively dependent on the outer metal shell. However, in our experiments, the exclusive precipitation of silver nanoparticles from TiO_2/Ag nanocomposites was observed as a result of insufficient TiO_2 support concentration.

TEM investigations of many nanocomposite samples revealed the presence of characteristic assemblies, such as those shown in Figure 1F, regardless of the silver particles size and/or morphology. Most TiO_2 nanorods appear to disperse in close proximity to the Ag nanoparticles by orienting their shortest side toward the surface of the metal cluster. Some considerations may be proposed in order to explain such a particle arrangement, as summarized in Scheme 1.

It is premised that the TiO_2 nanorods used in this work result from the dynamic restructuring of the surfactant molecules in the growing OLEA/TTIP mixtures.[23] Anisotropic crystal growth is likely promoted by a face-selective OLEA adsorption on the TiO_2 nanocrystals. In agreement with this mechanism, as the resulting TiO_2 nanorods elongate along the *c*-axis direction of the anatase lattice, it can be inferred that atoms belonging to the ⟨004⟩ surface planes (perpendicular to the *c*-axis) should be coordinated by OLEA molecules much less tightly than those bound to other faces (Scheme 1, step 1). With respect to the nanocomposite synthesis, this fact might imply that, in correspondence with the ends (short side) of the nanorods, more favorable local conditions for silver deposition occur, possibly due to an easier surfactant desorption and/or to a relatively reduced number of organic-passivated surface sites when compared to other faces (Scheme 1, step 2). Moreover, it has been demonstrated that there are remarkable differences in the Ag deposition quantum yields for TiO_2 surfaces with different crystallographic orientations, deriving from surface or near-surface structure characteristics rather than from the bulk crystal structure.[26] In this respect, a higher reactivity for the ⟨004⟩ exposed planes might be invoked as a factor enhancing the probability of metal nucleation at the ends of the titania

(29) Sahyun, M. R. V.; Serpone, N. *Langmuir* **1997**, *13*, 5082.
(30) (a) Kolny, J.; Kornowski, A.; Weller, H. *Nano Lett.* **2002**, *2*, 361, and references therein. (b) Kamat, P. V.; Shanghavi, B. *J. Phys. Chem. B* **1997**, *101*, 7675. (c) Westcott, S. L.; Oldenburg, S. J.; Lee, R.; Halas, N. J. *Langmuir* **1998**, *14*, 5396.

Scheme 1. Proposed Mechanism for the Colloidal Stabilization of Ag Nanoparticles by Means of TiO₂ Nanorods
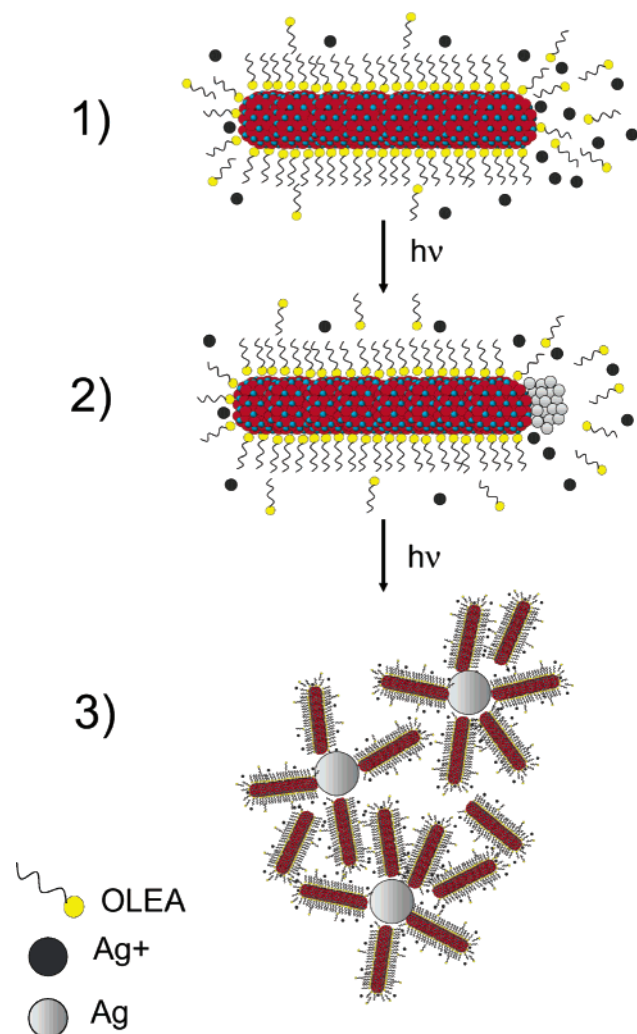
nanorods. In addition, specific electrostatic interactions might reasonably drive the nanorods to dynamically "coordinate" to the silver particles by assuming a more favorable orientation with respect to their surface (Scheme 1, step 3). As a matter of fact, such TiO₂ adsorption on Ag through ⟨004⟩ surface planes was demonstrated to be sufficiently strong to make the silver particles stable against centrifugation. As a confirmation, treatment aiming to destabilize the sole TiO₂ nanorods, such as addition of large volumes of a nonsolvent (MeOH or EtOH), determined the simultaneous precipitation of the silver particles, thus proving their intimate interactions with titania.

In summary, a mechanism for the colloidal stabilization of the silver nanoparticles may be supposed, which allows one to regard the TiO₂ nanorods as inorganic stabilizers, thus acting in the same manner as conventional surfactant molecules do.

(4.3) Evolution of the Optical and Morphological Features of the Ag Nanoparticles. The surface plasmon band of metals is known to strongly depend on the particle size and shape, on the refractive index of the surrounding medium, and on the nature of absorbed species.[1,10–13] In principle, silver sols prepared under different conditions can often exhibit quite different absorption spectra although the particle size distributions appear similar.[10a]

During the course of UV irradiation of deaerated TiO₂/AgNO₃

solution, a characteristic evolution of the silver plasmon band was observed (Figure 2). In other reports in which the reduction reaction was slow enough to be monitored during time,[15a,d,g,j] the Ag plasmon maximum was seen to blue-shift, the bandwidth to decrease, and the absorbance magnitude to become higher for particles increasing their size. Such behavior was basically related to depletion of chemiadsorbed Ag⁺ ions onto the particle surface with Ag⁺ reduction proceeding to completion.

In our work, the absorption changes observed at intermediate times of UV exposure (Figure 2b–f) were associated to a progressive size shrinking and a narrowing of the size distribution (Figure 1C,D) after the initial formation of very large particles (cfr. Figure 1B). An unstructured plasmon absorption, which was extremely low in magnitude and extended through the whole visible range was exclusive to large (20–50 nm) and agglomerated faceted Ag particles, whereas uniformly sized spherical nanoparticles ($d \approx 10$ nm) exhibited a comparatively more intense, narrow, and symmetric SP band with a remarkably blue-shifted λ_{max} (at about 410 nm). Accordingly, larger (20–50 nm) but well-separated Ag particles with a wide shape distribution were found at very long irradiation times (Figure 1E) which exhibited a broader and red-shifted ($\lambda_{max} \approx 430$ nm) SP band. Aggregation among clusters and broad size distribution are known to cause a broadening and dampening of the plasmon band. Hence, the plasmon band evolution in our experiments reflects the variation of the silver mean particle size and size dispersion, as predicted for metal particles in the extrinsic size region.[1,10,15,16]

Notably, the final λ_{max} for Ag particles of a certain dimension was red-shifted with respect to the position for the correspondent standard aqueous silver colloid. Two major factors are responsible for this red shift, in the absence of surface ligands for silver: the higher refractive index of the solvent ($n_{CHCl_3} = 1.445$, $n_{EtOH} = 1.361$ as compared with $n_{H_2O} = 1.333$),[10a,15f–h] and the presence of a TiO₂ environment ($n_{TiO_2} = 2.55$ for anatase)[11c,22c,d] which further increases the local refractive index around the silver particle surface.

The Ag nanoparticles were identified in three distinctive stages during their photochemical size/morphological conversion. At the very beginning of the photoreduction process, large silver particles (15–60 nm) were formed, most likely by coalescence of smaller clusters or by seed-mediated growth processes,[15b,c] as expected from the absence of a strong repelling layer of organic stabilizers. For the same reason, aggregation was also prone to occur.

At intermediate exposure times, the situation was gradually seen to change toward an increase of the population of smaller particles (∼10 nm). This conversion was seen to occur also for preformed large Ag particles prepared by conventional borohydride reduction and subsequently subjected to UV-light in deaerated solutions. Although small Ag clusters have been previously obtained by short laser illumination of preformed larger particles,[31a–c] they have been also reported upon irradia-

(31) (a) Kamat, P. V.; Flumiani, M.; Hartland, G. V. *J. Phys. Chem. B* **1998**, *102*, 3123. (b) Ah, C. S.; Han, H. S.; Kim, K.; Jang, D.-J. *J. Phys. Chem. B* **2000**, *104*, 8153. (c) Ah, C. S.; Han, H. S.; Kim, K.; Jang, D.-J. *Pure Appl. Chem.* **2000**, *72*, 91. (d) Linnert, T.; Mulvaney, P.; Henglein, A. *Ber. Bunsen-Ges Phys. Chem.* **1991**, *95*, 838. (e) Murakoshi, K.; Tanaka, H.; Sawai, Y.; Nakato, Y. *J. Phys. Chem. B* **2002**, *106*, 3041.
(32) (a) Henglein, A. *Chem. Rev.* **1989**, *89*, 1861. (b) Henglein, A. *J. Phys. Chem.* **1993**, *97*, 5457. (c) Henglein, A. *Ber. Bunsen-Ges. Phys. Chem.* **1977**, *81*, 556. (d) Henglein, A. *Elektrochemie der Metalle*; DECHEMA Monographien; Wiley-VCH: Weinheim, Germany, 1983; Vol. 93, p 163.

tion with low-intensity UV sources.[10d,e] In agreement with the former studies, photofragmentation can be assumed to be the most likely mechanism for Ag size decrease, involving the break-up of metal clusters which have accumulated sufficient charge at or near the metal surface upon UV-induced photo-ejection of electrons.[31a] Although photodissolution might concurrently occur to some extent through hole oxidation, this process is not considered significant in the present experiments.

The latest stages of Ag particle conversion were, in fact, characterized by the renewed observation of bigger clusters, although not agglomerated and well-dispersed, with a mixture of faceted and rodlike particles (Figure 1E). These modifications, however, required a much longer time frame to occur with respect to all preceding changes. This latter conversion is believed to be essentially driven by light-induced ripening processes, similar to that occurring during the phototransformation of small spherical nanoparticles into large nanoprisms.[10d–g]

In general, the time required to detect well-defined particle features becomes longer with increases in the starting $AgNO_3$ concentration, as absorption of a higher number of photons is required to induce the photomodification of a higher concentration of silver clusters.

The above-reported observations suggest that the proposed approach provides a simultaneous tool both for yielding stable colloidal Ag nanoparticles and for somehow modulating the average metal particle size and size distribution by the exclusive use of light.
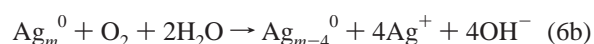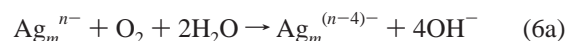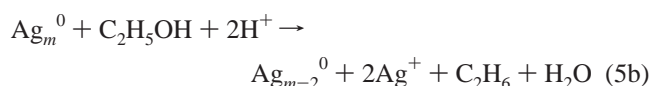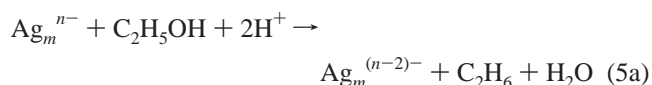
(4.4) Redox Properties of the Nanocomposites. The results shown in Figure 3 highlighted that the as-prepared Ag nanoparticles are sensitive to air. Throughout the bleaching process, the solution remained transparent without developing any turbidity. This fact primarily indicated that the decrease of the silver plasmon band was not due to agglomeration among the particles. The UV–vis spectra, in fact, confirmed that the bands remained rather symmetrical without showing any sign of scattering. Consequently, discoloration was caused either by oxidation of silver particles or by plasmon damping. The necessity of ambient atmosphere for the bleaching process pointed to oxidative dissolution, as damping is an oxygen-independent phenomenon. This explanation was corroborated by the observation that, under nitrogen, only a little bleaching and a small red shift were seen, after which the plasmon bands remained practically identical. Such red-shift and absorbance decrease were qualitatively similar to those detected in the early stages of exposition to air (Figure 3a–d), except for occurring much more slowly.

The pronounced reactivity of the metal nanoparticles can be understood as arising from two conditions. First, the absence of a compact organic surface layer does not protect them from oxidation,[35] and, second, the silver redox potential is shifted to negative values (i.e. far below the conventional electrode value of +0.779 V) with decreasing particle size.[7a,15d,32] In addition, silver clusters are known to be able to store electrons upon charge injection from reducing species. Accordingly, their

Fermi level is displaced to even more negative potentials than in uncharged particles.

The initial minor absorption decrease accompanied by a SP red shift in Figure 3 can be attributed to the discharge of excess electrons (injected by e_{CB}^- and/or reductive radicals) either to the solvent[4e,15d,g,22b] (eq 5a) in N_2-saturated solutions or to both the solvent and dissolved oxygen (eq 6a) in aerated solutions. Both the standard potentials $E^0 = +0.46$ V for C_2H_5OH/C_2H_6 and $E^0 = +0.4$ V for O_2/OH^- are favorable toward oxidation of the silver nanoparticles (designated as Ag_m).

Undoubtedly, O_2 was responsible for dissolving (eq 6b) the silver particles,[15j,22a] as inferred by the progressive bleaching and the concomitant blue shift of the SP band (Figure 3e–n) that occurred under air. However, silver oxidation by ethanol (eq 5b) was much less important than the route involving O_2, as proven by the occurrence of negligible dissolution under air-free conditions on a comparable time scale. Accordingly, Ag deposits have already been reported to be relatively poor catalysts for ethanol reduction, due to the nonohmic nature of silver.[4e]

$$Ag_m^{n-} + C_2H_5OH + 2H^+ \rightarrow$$
$$Ag_m^{(n-2)-} + C_2H_6 + H_2O \quad (5a)$$

$$Ag_m^0 + C_2H_5OH + 2H^+ \rightarrow$$
$$Ag_{m-2}^0 + 2Ag^+ + C_2H_6 + H_2O \quad (5b)$$

$$Ag_m^{n-} + O_2 + 2H_2O \rightarrow Ag_m^{(n-4)-} + 4OH^- \quad (6a)$$

$$Ag_m^0 + O_2 + 2H_2O \rightarrow Ag_{m-4}^0 + 4Ag^+ + 4OH^- \quad (6b)$$

With regard to $CHCl_3$, the polarographic half-wave potential of $CHCl_3$, which can be ascribed to the process

$$CHCl_3 + H_2O + 2e^- \rightarrow CH_2Cl_2 + Cl^- + OH^- \quad (7)$$

is reported at −1.46 V (vs NHE).[33] As the standard potential E^0 for Ag^+/Ag_m^0 abruptly increases[32] from −1.8 V for $m = 0$ to −0.9 V (vs NHE) for $m = 3$, this implies that even Ag clusters that are much smaller than our nanoparticles would not be oxidized by $CHCl_3$.

When Ag^+ ions are formed, the Fermi level in the silver nanoparticles should move to a more positive potential, thus somehow decreasing the driving force for oxidation, provided that Ag^+ concentration around the silver clusters is high enough. This actually was proven by experiments in which fresh addition of $AgNO_3$ to preformed TiO_2/Ag colloids suppressed oxidation to a considerable extent.

The experiments in which excess $NaBH_4$ was added to a solution of photocatalytically prepared TiO_2/Ag nanocomposites (Figure 4) indicated that the metal particles were catalytically active. The detected spectral changes, although qualitatively similar to those in Figure 2b–f, were, however, due to a completely different phenomenon. A variation of the silver particle size was, in fact, not observed in this case. Excess electrons injected into the particles[10a] can produce characteristic SP changes, as previously reported.[10e,22b] However, on the basis of the extremely pronounced blue shift and band sharpening, it is evident that the surface negative charge density on the silver

(33) Kolthoff, I. M.; Lee, T. S.; Stocesova, D.; Parry, E. P. *Anal. Chem.* **1950**, *22*, 251.
(34) (a) Jana, N. R.; Pal, T. *Langmuir* **1999**, *15*, 3458. (b) Sau, T. K.; Pal, A.; Pal, T. *J. Phys. Chem. B* **2001**, *105*, 9266. (c) Li, Y.; Boone, E.; El-Sayed, M. A. *Langmuir* **2002**, *18*, 4921.
(35) Aoki, K.; Chen, J.; Yang, N.; Nagasawa, H. *Langmuir* **2003**, *19*, 9904.

particles is increased from the value attained by electron injection from e_{CB}^- and/or reductive radicals upon UV– photoexcitation of TiO₂. This can be explained by considering the high nucleophilicity of NaBH₄ ($E^0 = -1.3$ V vs NHE). The discharging process occurred in accordance with the processes described by eqs 5 and 6. Nevertheless, the metal dissolution rate was much slower in these experiments, likely due to depletion of dissolved oxygen as long as an excess of borohydride was present in the solution. This latter observation seems to contradict other reported results[15j] in which a higher susceptibility to oxidation was instead invoked to explain the reversible Ag nanoparticle formation in the presence of excess borohydride. However, the presence of strong surfactants for Ag⁺ ions was a stringent requirement to observe the oxygen-driven dissolution in that case.

From all the above observations, it can be seen that the photocatalytically synthesized TiO₂-stabilized Ag nanoparticles actually possess an intrinsic high reactivity. They can either serve as reductants by themselves or act as mediators in redox processes[1,7,34] where their inherent redox potential can eventually be tuned by varying the particle size, as emphasized in many studies.[6a,b,7a,c,21b,34] Silver nanoparticles can indeed store electrons; however, oxygen-free conditions are required to both preserve the surface charge and the particle size, as these two latter determine the overall metal particle redox potential. The slow discharge of the accumulated electrons into the solution under deaerated conditions can be advantageous in that the reduction of a target substrate would not compete with the solvent reduction.

For use in TiO₂-based photocatalysis, analogous oxygen-free conditions are required to prevent metal photodissolution. In this application, the silver particles could promote charge carrier separation while also mediating an electron-transfer process. In addition, the overall catalytic activity for the nanocomposite can be expected to be related to the above-recognized light-induced size-morphological modifications of the metal particles. This fact should be taken into account in photocatalytic studies, as it may give rise to a TiO₂/Ag nanocomposite photocatalyst whose catalytic activity varies continuously[34] as a function of the metal particle size during the course of steady-state photocatalysis.

5. Conclusions

The simple photocatalytical preparation of a novel Ag/TiO₂ nanocomposite system in optically clear apolar solutions has been demonstrated in the presence of surfactant-capped anatase TiO₂ nanorods as stabilizers for the silver particles. The size-morphological features of the metal nanoparticles can be controlled by varying the irradiation time. It is believed that a finer tuning of the silver particle size could eventually be achieved by careful adjustment of the irradiation conditions, as recently demonstrated by means of selective plasmon excitation.[10d–g]

The proposed approach offers a novel method for producing highly reactive silver nanoclusters with "clean" surfaces, thus potentially useful for applications in sensing devices and in homogeneous redox catalysis and photocatalysis.

At present, experiments are in progress in our laboratories to assess the performance of the TiO₂/Ag nanocomposite in steady-state photocatalysis.